Detection of interstellar H_2D^+ emission

Ronald Stark

Max-Planck-Institut für Radioastronomie, Auf dem Hügel 69, D-53121 Bonn, Germany

and

Floris F.S. van der Tak & Ewine F. van Dishoeck

Sterrewacht Leiden, Postbus 9513, NL-2300 RA Leiden, The Netherlands

Accepted for publication (June 11, 1999) in the Astrophysical Journal (Letters)

ABSTRACT

We report the detection of the $1_{10}-1_{11}$ ground state transition of ortho-H_2D^+ at 372.421 GHz in emission from the young stellar object NGC 1333 IRAS 4A. Detailed excitation models with a power-law temperature and density structure yield a beam-averaged H_2D^+ abundance of 3×10^{-12} with an uncertainty of a factor of two. The line was not detected toward W 33A, GL 2591, and NGC 2264 IRS, in the latter source at a level which is $3-8$ times lower than previous observations. The H_2D^+ data provide direct evidence in support of low-temperature chemical models in which H_2D^+ is enhanced by the reaction of H_3^+ and HD. The H_2D^+ enhancement toward NGC 1333 IRAS 4A is also reflected in the high DCO^+/HCO^+ abundance ratio. Simultaneous observations of the N_2H^+ $4-3$ line show that its abundance is about $50-100$ times lower in NGC 1333 IRAS 4A than in the other sources, suggesting significant depletion of N_2. The N_2H^+ data provide independent lower limits on the H_3^+ abundance which are consistent with the abundances derived from H_2D^+. The corresponding limits on the H_3^+ column density agree with recent near-infrared absorption measurements of H_3^+ toward W 33A and GL 2591.

Subject headings: ISM: abundances — ISM: molecules — molecular processes — radio lines: ISM — submillimeter

1. Introduction

The recent detection of the H_3^+ ion in interstellar clouds through its infrared vibration-rotation lines (Geballe & Oka 1996; McCall et al. 1998) is an important confirmation of the gas-phase chemical networks (Herbst & Klemperer 1973; Watson 1973). Because of its symmetry, H_3^+ has no allowed rotational transitions contrary to its deuterated isotopomer H_2D^+ which has a large permanent dipole moment (Dalgarno et al. 1973). Thus, H_2D^+ is important as a tracer of H_3^+ with transitions that can be searched for in emission. In addition, it is widely believed to play a pivotal role in the interstellar ion-molecule chemistry at low temperatures where significant enhancement of deuterated molecules occurs as a result of fractionation (e.g. Herbst 1982; Millar et al. 1989). This process is initiated by the isotope exchange equilibrium reaction $H_3^+ + HD \rightleftharpoons H_2D^+ + H_2$ (1) which is shifted in the forward direction at low temperatures (Smith et al. 1982; Herbst 1982). The formation of H_2D^+ is followed by deuterium transfer reactions with e.g. CO to form DCO^+, and the H_2D^+ enhancement is reflected in the observed large abundance ratios of e.g. DCO^+/HCO^+, NH_2D/NH_3, and DCN/HCN in cold clouds (e.g. Wootten 1987; Butner et al. 1995; Williams et al. 1998).

Over the last 20 years numerous attempts have been made to detect the $1_{10} - 1_{11}$ ortho-H_2D^+ and $1_{01} - 0_{00}$ para-H_2D^+ ground state lines at 372 and 1370 GHz, respectively. These searches have mainly been done with the *Kuiper Airborne Observatory* (KAO) (Phillips et al. 1985; Pagani et al. 1992a; Boreiko & Betz 1993), and a possible absorption feature at 1370 GHz has been reported by Boreiko & Betz (1993) toward Orion. Observations from the ground are very difficult since the 372 GHz line is at the edge of a strong atmospheric water absorption line, while the atmosphere at 1370 GHz is almost completely opaque. With the advent of new submillimeter receivers equipped with sensitive niobium SIS mixers it has become possible to search for weak ortho-H_2D^+ lines from high, dry sites such as

Mauna Kea. Indeed, a ground-based search for this line from the *Caltech Submillimeter Observatory* (CSO) by van Dishoeck et al. (1992) yielded limits which are up to a factor of hundred more sensitive than those obtained with the KAO. Comparison with chemical models suggested that only a factor of a few improvement would be needed to detect the line. With the new facility receiver RxB3 at the *James Clerk Maxwell Telescope* (JCMT)[1] such an improvement in sensitivity is now achievable. Here we report the detection of the H_2D^+ 372.421 GHz line toward NGC 1333 IRAS 4A and significant upper limits toward W 33A, GL 2591, and NGC 2264 IRS. Simultaneous observations of the N_2H^+ $4-3$ line at 372.672 GHz toward these young stellar objects (YSOs) are used to place additional constraints on the H_3^+ abundance.

2. Observations

The observations of the $1_{10}-1_{11}$ ground state transition of ortho-H_2D^+ at 372.42134 GHz (Bogey et al. 1984) were done with the JCMT on August 31, September 15 and 18, 1998 during three nights of very good submillimeter transparency with a zenith opacity at 225 GHz below 0.05. The dual-polarization heterodyne receiver RxB3 was used (Avery 1998). Both mixers were tuned to 372.5469 GHz in the upper sideband. The big advantage of RxB3 is that it has a dual-beam interferometer which allows single-sideband (SSB) operation, enhancing the sensitivity and calibration at 372 GHz considerably. The digital autocorrelator spectrometer (DAS) was split into four parts of 125 MHz. This setup allows observations of both lines in two orthogonal polarizations simultaneously with a spectral

---

[1]The JCMT is operated by the Joint Astronomy Centre in Hilo, Hawaii on behalf of the Particle Physics and Astronomy Research Council in the United Kingdom, the Netherlands Organisation for Scientific Research, and the National Research Council of Canada.

resolution of 376 kHz ($\equiv$ 0.3 km s^{-1} at 372 GHz). Typical SSB system temperatures including atmospheric losses were about 1200 K. The effective total integration time was 7 hours on NGC 1333 observed over two nights, 2.7 hours on W 33A, 4.3 hours on GL 2591, and 4 hours on NGC 2264. The absolute calibration uncertainty is estimated at 30%, and the relative calibration between the H_2D^+ and N_2H^+ lines is much better. The JCMT beamsize at 372 GHz is 13$''$ FWHM, the main beam efficiency is 57%. JCMT data on $H^{13}CO^+$ and DCO^+ were taken from the literature (see below), except for DCO^+ toward W 33A and GL 2591, for which the $3-2$ transition at 216.113 GHz was observed with receiver RxA3. The beamsize at this frequency is 21$''$ FWHM and the main beam efficiency is 70%.

The observed H_2D^+ and N_2H^+ spectra are presented in Figure 1. The source and line parameters are listed in Table 1. The H_2D^+ line is clearly detected with $T_A^* = 0.08 \pm 0.03$ K toward NGC 1333 IRAS 4A, and is seen in spectra of both nights. The velocity width shows good agreement with the N_2H^+ line width while the velocities are offset by about 0.5 km s^{-1}. Comparison with the line survey of Blake et al. (1995) shows that such an offset is small and common for this region. No H_2D^+ emission was detected toward NGC 2264 IRS, W 33A, and GL 2591. Assuming the same width as the N_2H^+ line, 2σ upper limits of $T_A^* \leq 0.02 - 0.04$ K are obtained. For NGC 2264 this limit is about a factor of eight below the possible feature of Phillips et al. (1985), and a factor of three below the limit reached by van Dishoeck et al. (1992). Note that the N_2H^+ emission toward NGC 1333 is much weaker than that toward the other sources. No other lines were detected in the 125 MHz bands.

3. Analysis

Model calculations were performed to determine the abundances of H_2D^+, N_2H^+, HCO^+, and DCO^+ using a power-law density structure $n = n_0(r/R_o)^{-\alpha}$, as described in van der Tak et al. (1999). In these models the radial dust temperature profile is calculated from the observed luminosity and n_0 is determined from submillimeter photometry, which probes the total dust mass. The grain heating and cooling are solved self-consistently as a function of radius, r, using grain properties from Ossenkopf & Henning (1994). The outer radius (R_o) is determined from high resolution submillimeter line and continuum maps. The exponent α is constrained by modeling the relative strength of emission lines of CS and H_2CO at the central position over a large range of critical densities with a Monte Carlo radiative transfer program, assuming $T_{\rm K} = T_{\rm dust}$. Data were taken from Blake et al. (1995) (NGC 1333 IRAS 4A), de Boisanger et al. (1996) and Schreyer et al. (1997) (NGC 2264 IRS), and van der Tak et al. (1999 and in preparation) (GL 2591 and W 33A). For NGC 1333 IRAS 4A, where CS is heavily depleted, $\alpha = 2$ was taken based on the analysis of the continuum visibilities in interferometer data by Looney (1998).

Given the calculated temperature and density structure, the radiative transfer models were run to determine the abundances, assuming initially a constant abundance throughout the envelope. Both the ortho-H_2D^+ and para-H_2D^+ ladders have been considered since their spin states are coupled through reactive collisions with H_2; thus the para 0_{00} level is the true rotational ground state. A de-excitation rate coefficient of 1.0×10^{-10} cm^3 s^{-1} has been used for all inter-ladder transitions. See Herbst (1982) and Pagani et al. (1992b) for a detailed study of the ortho/para ratio. The lower level of the $1_{10} - 1_{11}$ transition lies at 86 K. The excitation energy of the 1_{10} level is 18 K relative to the 1_{11} level, and the critical density for this transition is about 2×10^5 cm^{-3}.

The calculated abundances are listed in Table 2. Toward NGC 1333 we infer a beam-averaged abundance $x(\mathrm{H_2D^+}) = 3 \times 10^{-12}$. Upper limits on the abundance toward NGC 2264, W 33A, and GL 2591 are $< 1 \times 10^{-11}$. The $\mathrm{N_2H^+}$ abundance ranges between 10^{-11} toward NGC 1333 and 10^{-9} toward W 33A. All derived abundances have an absolute uncertainty of a factor of two, due to the uncertainties in the dust opacities and CO abundances. The relatively high $\mathrm{N_2H^+}$ abundance toward NGC 2264 was already found by van Dishoeck et al. (1992), who noted that nearly all of the gas phase nitrogen must be in the form of $\mathrm{N_2}$ in this cloud. Since $\mathrm{N_2H^+}$ is formed mainly by the reaction of $\mathrm{H_3^+}$ and $\mathrm{N_2}$, the latter observations provide an independent lower limit on the $\mathrm{H_3^+}$ abundance. Destruction occurs mainly via reactions with CO, O, and electrons. Considering CO destruction only, $n(\mathrm{H_3^+}) \gtrsim 0.5\, n(\mathrm{N_2H^+})\, x(\mathrm{CO})/x(\mathrm{N_2})$ (2). Assuming 50% of the nitrogen is in $\mathrm{N_2}$, $x(\mathrm{N_2}) = 5 \times 10^{-5}\delta(\mathrm{N_2})$, $x(\mathrm{CO}) = 2 \times 10^{-4}\delta(\mathrm{CO})$ and equal amounts of depletion δ for CO and $\mathrm{N_2}$, this yields $x(\mathrm{H_3^+}) \gtrsim 2x(\mathrm{N_2H^+})$. These limits are listed in Table 2, and are consistent with the upper limits derived from the $\mathrm{H_2D^+}$ observations using a theoretical $\mathrm{H_2D^+/H_3^+}$ ratio, see §4.

4. $\mathrm{H_2D^+/H_3^+}$ chemistry

The above analysis assumes constant abundances throughout the YSO envelopes. In reality, the $\mathrm{H_2D^+}$ abundance is a strong function of temperature and position. In chemical equilibrium, the $\mathrm{H_3^+}$ abundance can be written as $x(\mathrm{H_3^+}) = \zeta/\Sigma k_\mathrm{X} n(\mathrm{X})$ with $n(\mathrm{X}) = n(\mathrm{H_2})x(\mathrm{X})$. X refers to any of O, C, CO, $\mathrm{O_2}$, $\mathrm{N_2}$, $\mathrm{H_2O}$, ... which are the principal removal agents of $\mathrm{H_3^+}$ via the proton transfer reactions $\mathrm{H_3^+} + \mathrm{X} \rightarrow \mathrm{XH^+} + \mathrm{H_2}$ (3), where k_X are the rate coefficients (taken from the UMIST database, see e.g. Millar et al. 1997) and ζ is the cosmic-ray ionization rate (taken to be 5×10^{-17} s^{-1}). A simple chemical model for the formation and destruction of $\mathrm{H_2D^+}$ yields

$$\frac{x(\mathrm{H_2D^+})}{x(\mathrm{H_3^+})} = \frac{x(\mathrm{HD})k_f + x(\mathrm{D})k_D}{x(e)k_e + \sum k_X x(\mathrm{X}) + k_r}, \tag{4}$$

where k_f and k_r are the forward and backward rate coefficients of reaction (1), k_D is the rate coefficient for formation of H_2D^+ through the reaction $H_3^+ + D$, and k_e is the rate coefficient of the electron recombination of H_2D^+ (see e.g. Caselli et al. 1998 for a compilation of values). We assumed $x(HD) = 10x(D) = 2.8 \times 10^{-5}$ throughout.

The above H_3^+ and H_2D^+ chemical equations were included in the power-law models, and abundances at each position were calculated for the appropriate temperature and density. We have fixed the expression for k_r at $T < 20$ K to its value at 20 K, to ensure that $x(H_2D^+) < x(H_3^+)$ throughout. For simplicity, only X=CO was considered and the electron recombination was neglected. The CO depletion is inferred from $C^{17}O$ observations as described in van der Tak et al. (1999 and in preparation), and are listed in Table 2. For a homogeneous temperature and density structure, our model agrees well with the models of Millar et al. (1989) and Pagani et al. (1992b).

The power-law model results for NGC 1333 IRAS 4A are presented in Figure 2. Using these abundances, the H_2D^+ emission has been calculated, most of which originates from gas at $T = 25 - 35$ K. The model intensity agrees within 30% with that measured toward NGC 1333 IRAS 4A, and is consistent with the upper limit toward GL2591. They are a factor of $2 - 4$ larger than the upper limits toward NGC 2264 IRS and W 33A, respectively. Most likely, this small discrepancy results from effective removal of H_3^+ by other species than CO and/or by an overestimate of the size of the cloud. The H_3^+ column densities computed for W 33A and GL 2591 agree within a factor of $2 - 3$ with the directly observed column densities by Geballe & Oka (1996) and McCall et al. (1998). This good agreement between models and observations provides the strongest support for the basic H_3^+ and H_2D^+ chemical networks in dense, cold clouds.

The simple chemical networks described above (Eq. (2) and (3)) have also been used to model the N_2H^+ abundance from the N_2H^+/H_2D^+ ratio. Assuming equal amounts of depletion for CO and N_2, agreement within a factor of two between the measured and modeled N_2H^+ line intensities is obtained. The best fitting N_2 abundances are included in Table 2.

The derived H_2D^+/H_3^+ ratios are also compared with the observed DCO^+/HCO^+ ratios in Table 2. The enhancement in H_2D^+/H_3^+ is clearly reflected in the DCO^+/HCO^+ ratio, as expected since the latter species are directly formed by reactions of the former with CO. For NGC 1333 IRAS 4A, $DCO^+/HCO^+ = 0.5\ H_2D^+/H_3^+$, where the factor of 0.5 is consistent with the statistical branching ratio of 1/3 within the uncertainties. The DCO^+/HCO^+ ratio toward NGC 1333 IRAS 4A is a factor of $5-50$ higher than that toward the other sources. This can be explained by the difference in physical structure. In cold, dense (pre-)protostellar cores like NGC 1333 IRAS 4A where the CO and N_2 depletions are extreme, the H_2D^+ abundance is enhanced, because of the low temperature and because the main removal reactions of H_3^+ are suppressed. The H_2D^+ abundance will increase even stronger than that of H_3^+ since reaction (1) becomes the main destruction channel of H_3^+. In the case of NGC 2264, W 33A, and GL 2591, where the temperatures are higher and the depletion of CO and N_2 is less, reaction (3) becomes the main removal path of H_3^+.

The difference in physical structure may have its origin in the different stages of protostellar evolution. In particular, NGC 1333 IRAS 4A has been classified as a Class 0 object (André & Montmerle 1994), and is thus in a very early stage, with a large spatial separation between the quiescent and shocked regions (Blake et al. 1995).

5. Conclusions

With the current sensitivity of heterodyne receivers it is now possible to study the ortho-H_2D^+ $1_{10}-1_{11}$ 372.421 GHz line profile in emission in the early stages of star formation deep inside dense molecular clouds. Its importance lies in the fact that it is a tracer of H_3^+ and that it provides information on the deuterium abundance and temperature history of a cloud and on the chemical evolution during star formation. Further observations of the H_2D^+ and H_3^+ lines in a sample of very young Class 0 and Class I YSOs will therefore be very valuable.

Since the ortho-H_2D^+ ground state is at 86 K, the $1_{10} - 1_{11}$ line traces both the warm and cold regions, although the H_2D^+ enhancement will be strongest in the coldest regions. Observations of the $1_{01} - 0_{00}$ para-H_2D^+ ground state line at 1.37 THz toward the continuum of embedded YSOs may reveal cold H_2D^+ in absorption. The dual channel *German REceiver for Astronomy at THz frequencies* (GREAT) to be flown on the *Stratospheric Observatory For Infrared Astronomy* (SOFIA) would allow such observations. Combined with 372 GHz observations from the ground, the total abundance and the relative population of the ortho- and para-modifications may be determined which provides information on the formation, destruction, and excitation processes. Simultaneous deep observations of the HD $J = 1 - 0$ (2.7 THz) and para-H_2D^+ ground state lines toward YSOs may yield a direct measure of the (variation in) H_3^+ abundance over the cloud, and thus of the cosmic-ray ionization rate.

It is a pleasure to thank Lorne Avery for discussions and test observations at 372 GHz, Henry Matthews for the non-standard setup for the backend, and Leslie Looney and Lee Mundy for sharing their model results on NGC 1333 prior to publication. The observations would not have been possible without the flexible observing strategy of Remo Tilanus. Gerd-Jan van Zadelhoff, Fred Baas, and Jane Greaves did an excellent job in carrying out these observations in service. This work is supported by NWO grant 614.41.003.

REFERENCES

André, P. & Montmerle, T. 1994, ApJ, 420, 837

Avery, L.W. 1998, JCMT web page, <www.jach.hawaii.edu/JCMT/rx/b3/rxbman.html>

Blake, G.A., Sandell, G., van Dishoeck, E.F., et al. 1995, ApJ, 441, 689

Bogey, M., Demuynck, C., Denis, M., Destombes, J.L., & Lemoine, B. 1984, A&A, 137, L15

Boreiko, R.T. & Betz, A.L. 1993, ApJ, 405, L39

Butner, H.M., Lada, E.A., & Loren, R.B. 1995, ApJ, 448, 207

Caselli, P., Walmsley, C.M., Terzieva, R., & Herbst, E. 1998, ApJ, 499, 234

Dalgarno, A., Oppenheimer, M., & Berry, R.S. 1973, ApJ, 183, L21

de Boisanger, C., Helmich F.P., & van Dishoeck, E.F. 1996, A&A, 310, 315

Geballe, T.R., & Oka, T. 1996, Nat, 384, 334

Herbst, E. 1982, A&A, 111, 76

Herbst, E. & Klemperer, W. 1973, ApJ, 185, 505

Looney, L. 1998, PhD thesis, Univ. of Maryland

McCall, B.J., Hinkle, K.H., Geballe, T.R., & Oka, T. 1998, J.Chem.Soc.Far.Disc., 109, 267

Millar, T.J., Bennett, A., & Herbst, E. 1989, ApJ, 340, 906

Millar, T.J., Farquhar, P.R.A., & Willacy, K. 1997, A&AS, 121, 139

Ossenkopf, V., & Henning, Th. 1994, A&A, 291, 943

Pagani L., Wannier, P.G., Frerking, M.A., et al. 1992a, A&A, 258, 472

Pagani L., Salez M., & Wannier, P.G. 1992b, A&A, 258, 479

Phillips, T.G., Blake, G.A., Keene, J., Woods, R.C., & Churchwell, E. 1985, ApJ, 294, L45

Schreyer, K., Helmich, F.P., van Dishoeck, E.F., & Henning, Th. 1997, A&A, 326, 347

Smith, D., Adams, N.G., & Alge E. 1982, ApJ, 263, 123

van der Tak, F.F.S, van Dishoeck E.F., Evans, N.J., II, Bakker, E.J, & Blake, G.A. 1999, ApJ (in press)

van Dishoeck E.F., Phillips, T.G., Keene, J., & Blake, G.A. 1992, A&A, 261, L13

Watson, W.D. 1973, ApJ, 183, L17

Williams, J.P., Bergin, E.A, Caselli, P., Myers, P.C., & Plume, R. 1998, ApJ, 503, 689

Wootten, A. 1987, in Astrochemistry, IAU Symposium 120, eds. M.S. Vardya & S.P. Tarafdar (Kluwer, Dodrecht), p. 311

This manuscript was prepared with the AAS LaTeX macros v4.0.

Fig. 1.— Observed spectra of H_2D^+ $1_{10} - 1_{11}$ at 372.421 GHz and N_2H^+ $4-3$ at 372.672 GHz. The N_2H^+ spectra have a resolution of 0.3 km s^{-1}. The H_2D^+ spectra have been smoothed to 0.6 km s^{-1}.

Fig. 2.— Power-law model abundances of H_3^+, H_2D^+, and N_2H^+ as function of density and temperature.

Table 1. Observations[a]

Source[b]	Molecule	Transition	T_A^* (K)	ΔV (km s^{-1})	$V_{\rm LSR}$ (km s^{-1})
N1333	H_2D^+	$1_{10}-1_{11}$	0.08(0.03)	1.2 ± 0.3	7.4 ± 0.2
	N_2H^+	$4-3$	2.57(0.03)	1.35	6.94
N2264	H_2D^+	$1_{10}-1_{11}$	≤ 0.02[c]		
	N_2H^+	$4-3$	4.51(0.03)	2.67	8.01
W33A	H_2D^+	$1_{10}-1_{11}$	≤ 0.04[c]		
	N_2H^+	$4-3$	3.06(0.06)	4.62	37.40
GL2591	H_2D^+	$1_{10}-1_{11}$	≤ 0.02[c]		
	N_2H^+	$4-3$	1.41(0.04)	2.89	-5.82

[a]Values in parentheses represent 1σ statistical uncertainties. The absolute uncertainty of the intensity is 30%; ΔV and $V_{\rm LSR}$ are accurate to better than 0.1 km s^{-1}.

[b]Position (B1950): NGC 1333 IRAS4A: $\alpha = 03^{\rm h}26^{\rm m}04\overset{\rm s}{.}8$, $\delta = +31^\circ03'14''$; NGC 2264 IRS: $\alpha = 06^{\rm h}38^{\rm m}25\overset{\rm s}{.}0$, $\delta = +09^\circ32'29''$; W33A: $\alpha = 18^{\rm h}11^{\rm m}44\overset{\rm s}{.}2$, $\delta = -17^\circ52'56''$; GL 2591: $\alpha = 20^{\rm h}27^{\rm m}35\overset{\rm s}{.}8$; $\delta = +40^\circ01'14''$

[c]2σ limits: NGC 2264 IRS: $\Delta V = 2.5$, GL 2591: $\Delta V = 3.0$, and W33A: $\Delta V = 4.5$ km s^{-1}.

Table 2. Excitation model parameters and deduced abundances[a]

Source	α	n_0	T R_i, R_o	Molecular Abundances							
		(cm^{-3})	(K)	H_2D^+	N_2H^+	$H_3^{+\,b}$	$H_3^{+\,c}$	$\frac{H_2D^+}{H_3^+}$	$\frac{DCO^+}{HCO^+}$ [d]	CO[e]	N_2
N1333	2	1.7(6)	318, 13	3(−12)	1(−11)	2(−10)	> 2(−11)	2(−2)	1(−2)	4(−6)	4(−7)
N2264	1.5	1.5(4)	293, 18	< 1(−11)	6(−10)	< 3(− 9)	> 1(− 9)	< 3(−3)	3(−3)	6(−5)	4(−5)
W33A	1	2.1(4)	280, 16	< 1(−11)	1(− 9)	< 4(− 9)	> 2(− 9)	< 3(−3)	1(−4)	5(−5)	2(−5)
GL2591	1.25	3.5(4)	350, 30	< 1(−11)	5(−10)	< 3(− 9)	> 1(− 9)	< 3(−3)	4(−4)	2(−4)	9(−5)

[a]From statistical equilibrium calculations using the appropriate temperature and density structure as function of distance r to the YSO, $n(r) = n_o(r/R_o)^{-\alpha}$ where R_o is the outer radius of the model envelope: NGC 1333 IRAS 4A: 3.1(3) AU, NGC 2264 IRS: 4.7(4) AU, W33A: 2.4(5) AU, GL 2591: 3.1(4) AU, and $R_i = R_o/300$ is the inner radius. Notation a(b) indicates $a \times 10^b$. The accuracy of the deduced abundances is a factor of two.

[b]From H_2D^+ using a theoretical H_3^+/H_2D^+ ratio at the effective temperature from which most of the emission arises (see Figure 2).

[c]From N_2H^+ analysis (see text).

[d]From $H^{13}CO^+$ assuming $HCO^+/H^{13}CO^+ = 60$.

[e]From $C^{17}O$ assuming $CO/C^{17}O$=2500 and using the appropriate $N(H_2)$ from submillimeter dust emission in a 13″ beam: NGC 1333 IRAS 4A: 3.1(23) cm^{-2}, NGC 2264 IRS: 1.2(23) cm^{-2}, W 33A: 5.2(23) cm^{-2}, GL 2591: 1.3(23) cm^{-2}.

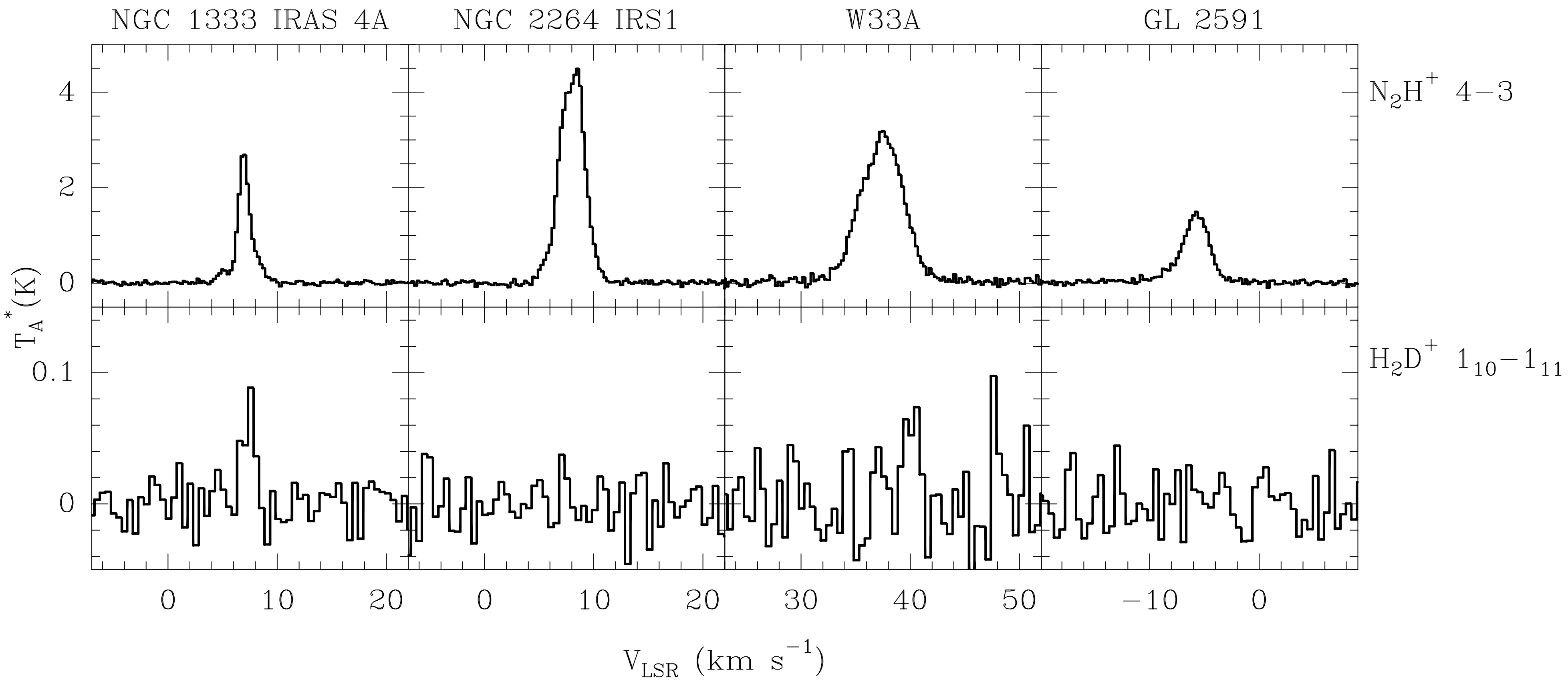
NGC 1333 IRAS 4A
NGC 2264 IRS1
W33A
GL 2591
N2H+ 4−3
H2D+ 1_10−1_11
T_A* (K)
V_LSR (km s^−1)
0
2
4
0.1
10
20
30
40
50
−10

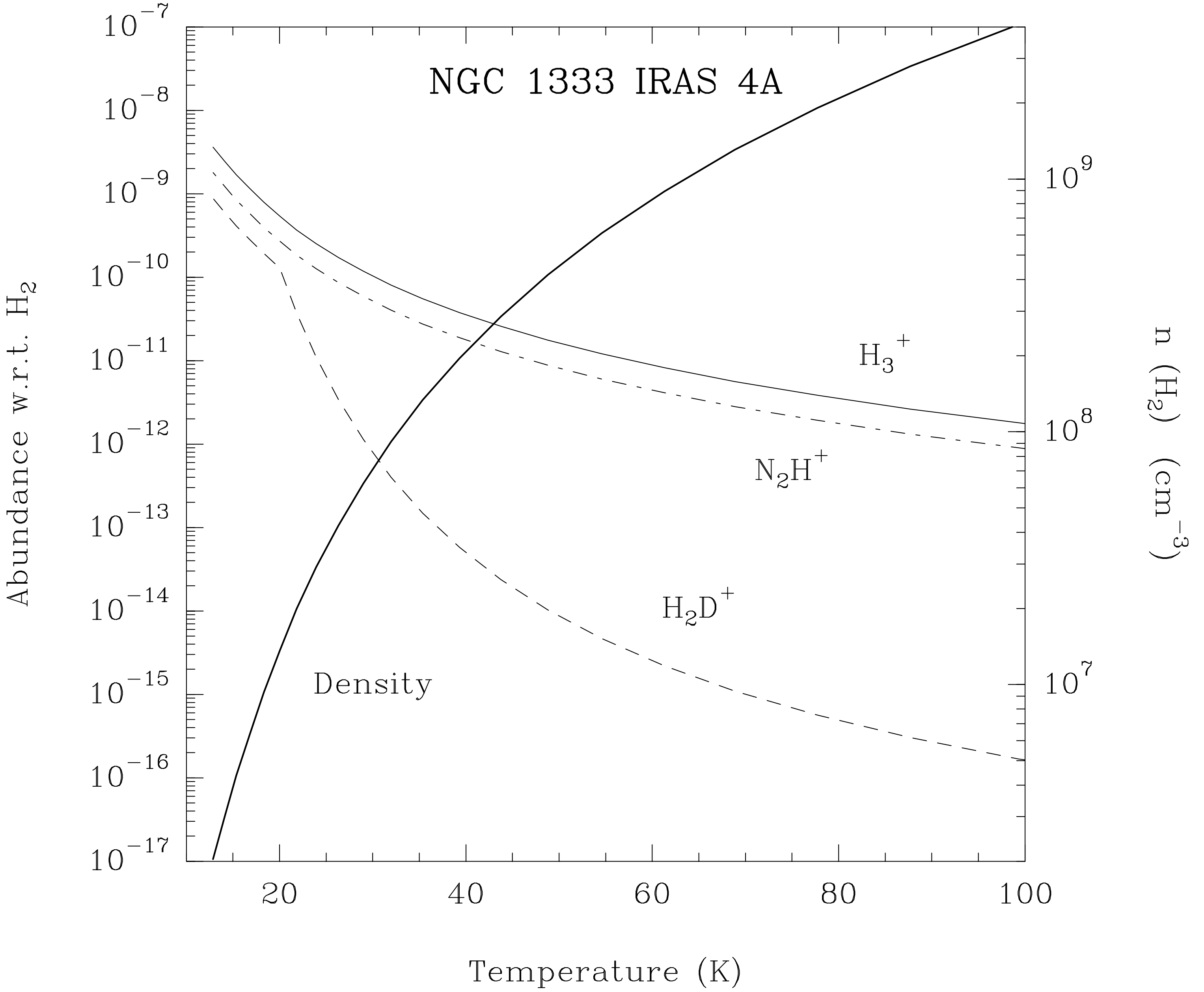
NGC 1333 IRAS 4A
Abundance w.r.t. H_2
10^{-7}
10^{-8}
10^{-9}
10^{-10}
10^{-11}
10^{-12}
10^{-13}
10^{-14}
10^{-15}
10^{-16}
10^{-17}
$n(H_2)$ (cm^{-3})
10^{9}
10^{8}
10^{7}
H_3^+
N_2H^+
H_2D^+
Density
20
40
60
80
100
Temperature (K)

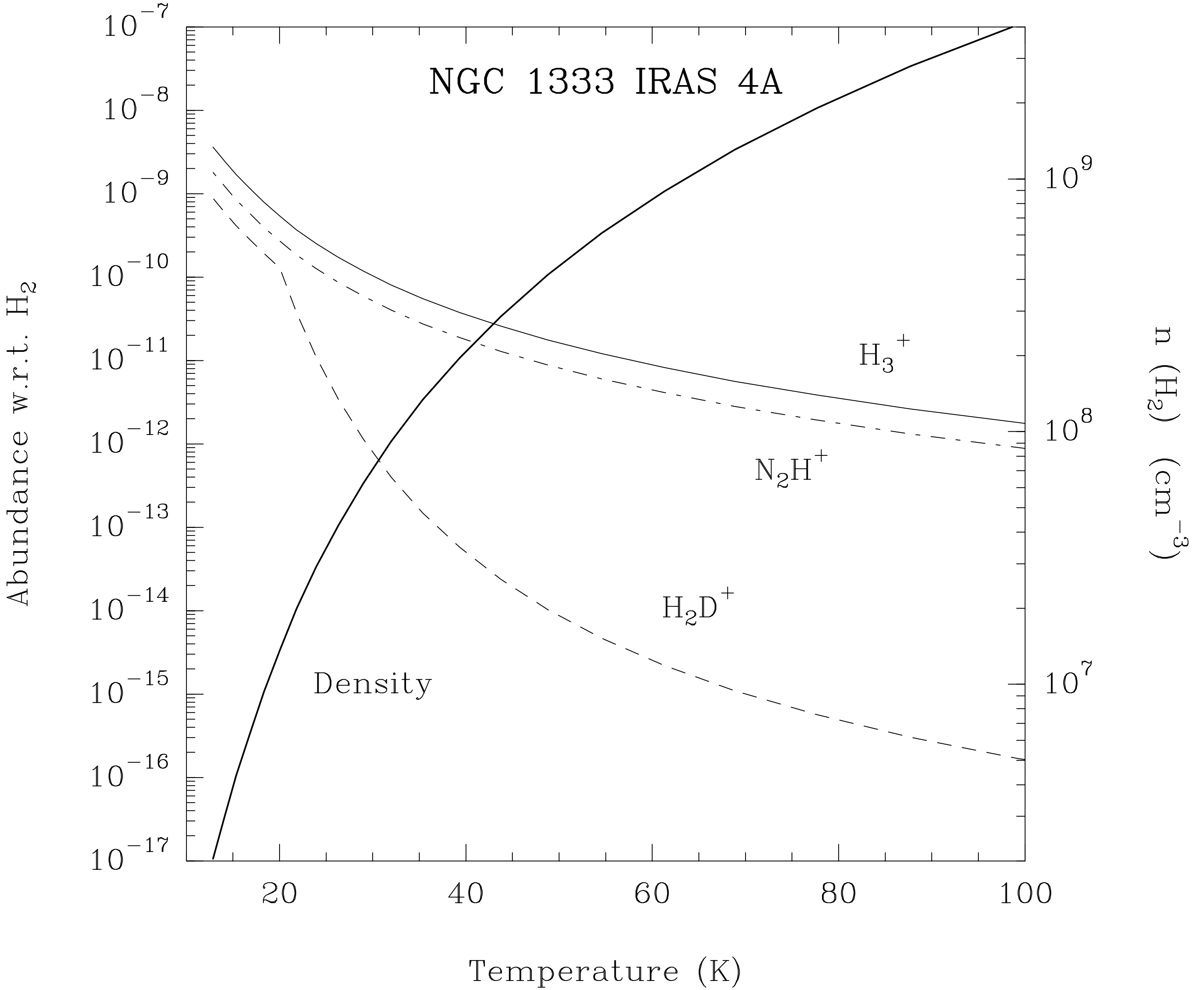

NGC 1333 IRAS 4A
Abundance w.r.t. H_2
$n\ (H_2)\ \ (cm^{-3})$
Temperature (K)
H_3^+
N_2H^+
H_2D^+
Density
10^{-7}
10^{-8}
10^{-9}
10^{-10}
10^{-11}
10^{-12}
10^{-13}
10^{-14}
10^{-15}
10^{-16}
10^{-17}
10^{9}
10^{8}
10^{7}
20
40
60
80
100